

See discussions, stats, and author profiles for this publication at: <https://www.researchgate.net/publication/231700693>

# Glassy Dynamics and Glass Transition in Thin Polymer Layers of PMMA Deposited on Different Substrates

ARTICLE *in* MACROMOLECULES · AUGUST 2010

Impact Factor: 5.8 · DOI: 10.1021/ma100912r

CITATIONS

48

READS

55

7 AUTHORS, INCLUDING:



**Emmanuel Mapesa**

University of Leipzig

23 PUBLICATIONS 300 CITATIONS

SEE PROFILE



**Anatoli Serghei**

Claude Bernard University Lyon 1

81 PUBLICATIONS 1,229 CITATIONS

SEE PROFILE



**Klaus Jochen Eichhorn**

Leibniz Institute of Polymer Research Dresden

180 PUBLICATIONS 2,785 CITATIONS

SEE PROFILE



**Friedrich Kremer**

University of Leipzig

302 PUBLICATIONS 6,182 CITATIONS

SEE PROFILE

# Glassy Dynamics and Glass Transition in Thin Polymer Layers of PMMA Deposited on Different Substrates

Michael Erber,<sup>†</sup> Martin Tress,<sup>‡</sup> Emmanuel U. Mapesa,<sup>‡</sup> Anatoli Serghei,<sup>§</sup>  
Klaus-Jochen Eichhorn,<sup>†</sup> Brigitte Voit,<sup>†</sup> and Friedrich Kremer<sup>\*‡</sup>

<sup>†</sup>Leibniz-Institute of Polymer Research Dresden e.V., 01069 Dresden, Germany, <sup>‡</sup>Institute for Experimental Physics I, University of Leipzig, 04103 Leipzig, Germany, and <sup>§</sup>Department of Polymer Science and Engineering, University of Massachusetts Amherst, Amherst, Massachusetts 01003

Received April 26, 2010; Revised Manuscript Received May 21, 2010

**ABSTRACT:** Spectroscopic vis-ellipsometry and broadband dielectric spectroscopy (BDS) are combined to study the glassy dynamics of thin ( $\geq 10$  nm) layers of atactic poly(methyl methacrylate) (PMMA) annealed and measured under *identical* conditions. In order to unravel a possible effect of the underlying substrate, the interfacial interactions are systematically modified ranging from strong attractive interactions for covalently bonded PMMA brushes with high grafting density and for native silicon oxide (Si/SiO<sub>x</sub>) to weak and strong repulsive interactions as realized by Au-coated and HMDS-treated Si/SiO<sub>x</sub> surfaces, respectively. Down to the thinnest analyzed PMMA layers and independently from the applied substrate, both methods deliver—within the experimental accuracy ( $\pm 1$  K for BDS and  $\pm 2$  K for ellipsometry)—a coinciding result. The glassy dynamics are *not* altered due to the one-dimensional confinement in these thin polymer layers. The results are discussed with respect to the highly controversial literature and the impact of the preparative conditions.

## 1. Introduction

The understanding of the mobility and dynamics of polymer chains near a surface is important for diverse technological applications as well as biological processes like adhesion and friction and DNA packaging in viruses, respectively. Consequently, the real nature of the effects of free surfaces and confinement on the glass transition—which remains an unresolved subject of polymer physics—has continued to attract considerable attention for more than a decade now.<sup>1–31</sup> Some of the factors that have been reported to influence the observed glassy dynamics include measurement ambients,<sup>1–3</sup> molecular weight,<sup>4,5</sup> tacticity of the polymer,<sup>6–9</sup> and the substrate surface.<sup>7,10–18</sup> Concerning the latter aspect, some reports<sup>13–16</sup> attribute an increase in  $T_g$  with reducing layer thickness to attractive polymer–substrate interfacial forces that are postulated to inhibit cooperative dynamics. On the other hand, repulsive or weak interfacial interactions have been held responsible for  $T_g$  depressions in confinement.<sup>10–12,14–16</sup>

In the present work, the expertise of two groups is harnessed—ellipsometry (at the IPF, Dresden) and BDS<sup>19</sup> (at the University of Leipzig)—to study the thickness dependence of glassy dynamics in atactic PMMA deposited on systematically modified substrate surfaces. By so doing, we have the advantage of combining a technique that measures macroscopic quantities (ellipsometry) with one which probes molecular fluctuations (BDS). To the best of our knowledge, such a study on *identically annealed and measured* samples of atactic-PMMA does not exist.

## 2. Experimental Section

**2.1. Sample Preparation.** Atactic-PMMA ( $M_w = 350\,000$  g/mol) with a narrow polydispersity of 1.05 and a calorimetric  $T_g$  of 393 K was used as received from Sigma-Aldrich (Germany). Highly polished (monocrystal 100) silicon wafers with a native silicon dioxide layer ( $\sim 2$  nm) served as substrates for both

ellipsometric and dielectric studies. Prior to layer deposition for ellipsometric measurements, the silicon surface was thoroughly purified with an alkaline cleaning procedure as described in the literature,<sup>20</sup> achieving—for the resulting surfaces—a static water contact angle  $\theta < 5^\circ$ . For the dielectric measurements, the first step was to evaporate an aluminum layer of  $\sim 70$  nm onto the backside to achieve a good electrical contact. Hence, to preserve this aluminum layer, the alkaline cleaning procedure was substituted by cleaning in ultrasonic baths of acetone and dichloromethane (“Chromasolv”, for HPLC) for at least 5 min each.

In order to modify the polarity of the hydrophilic Si/SiO<sub>x</sub> surfaces, different techniques were applied. In the first case, a thin ( $\sim 80$  nm) optically dense gold layer was vacuum-evaporated onto the purified Si/SiO<sub>x</sub> surface, thus achieving a water contact angle of  $75^\circ$  (a 3 nm thin Cr intermediate layer between SiO<sub>x</sub> and Au is applied as adhesive layer). In the second case, hexamethyldisilazane (HMDS) was used to modify the Si/SiO<sub>x</sub> surface as described elsewhere.<sup>21</sup> This silanization process resulted into a static water contact angle  $\theta$  of about  $90^\circ$ , indicating the hydrophobic modification of the surface with trimethylsilyl groups. In the third case, we sought to enormously increase the attractive interfacial interactions using PMMA brushes. Here, the polymer chains are covalently tethered to the Si/SiO<sub>x</sub> surface using the “grafting from” approach. Surface-initiated ATRP (atom transfer radical polymerization) was used to synthesize well-defined PMMA brushes (grafting density  $\sigma \sim 0.6$  chains nm<sup>-1</sup>).<sup>22</sup>

The PMMA layers were deposited on the different surfaces by spin-coating at a moderate rate of 3000 rpm (for 30 s) from filtered toluene solutions of the polymer. The thickness variation was achieved by varying the concentration of the solution.

**2.2. Sample Measurement and Data Analysis.** Temperature-dependent spectroscopic vis-ellipsometry measurements were carried out at a fixed angle of incidence of  $70^\circ$  using a multi-wavelength (370–1680 nm) rotating compensator ellipsometer (RCE) M2000VI (J.A. Woollam Co., Inc.) connected to a closed heat cell (INSTEC Inc.). The measurements were performed at a moderate rate of 2 K/min well above  $T_g$ , but below the polymer

\*Corresponding author. E-mail: kremer@physik.uni-leipzig.de.

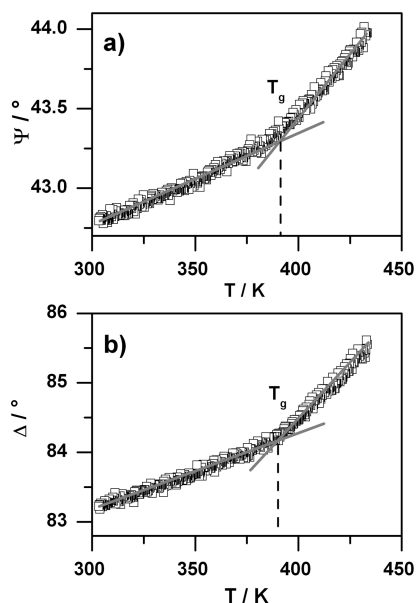


**Figure 1.** Ellipsometric angles  $\Psi$  and  $\Delta$  in dependence of temperature (first cooling scan) for a 67 nm thin PMMA layer on Si/SiO<sub>x</sub> at a sensitive wavelength of 450 nm. The gray lines are a guide to the eye to illustrate the two linear regimes whose intersection point indicates the glass transition temperature  $T_g$  as highlighted by the dashed line.

degradation temperature ( $T_{\text{onset}}$ : 500 K) as observed by thermogravimetric analysis. To avoid oxidation and degradation, which would otherwise occur at elevated temperatures, all measurements and annealing were performed *in situ* under dry argon (99.999% pure) flow. During annealing the thickness  $d$  and refractive index  $n$  of the sample were continuously monitored until an equilibrium conformation was reached (in at least 12 h at 430 K); then measurement would immediately commence. Values of  $d$  and  $n$  were fitted to the ellipsometric angles  $\Psi$  and  $\Delta$  (Figure 1) in the entire wavelength range assuming an appropriate layer stack as optical model. A Cauchy dispersion ( $k = 0$ ) for the wavelength dependence of the polymer refractive index was assumed. The temperature position of the discontinuity—commonly referred to as kink—in either  $d(T)$  or  $n(T)$  is known to occur at the (ellipsometrically determined) glass transition temperature,  $T_g$ . For a better accuracy,<sup>20</sup> the extremum of interpolated curves of the second derivatives of  $d(T)$  and  $n(T)$  were used to obtain  $T_g$ . An experimental uncertainty of  $\pm 2$  K is determined for all investigated systems.

The dielectric measurements were performed using a high-resolution Alpha Analyzer assisted by a Quatro temperature controller (both from Novocontrol Technologies GmbH) in a broad frequency domain (1 Hz–1 MHz) and at temperatures between 360 and 420 K (with an absolute error of  $\pm 1$  K). For these experiments, the PMMA layers were capped with a counter electrode covered with 550 nm high nanostructures acting as spacers (Figure 2a). This sample arrangement was recently developed and successfully adopted to circumvent the shortcomings of conventional evaporated electrodes.<sup>23,24</sup> Each sample was annealed for at least 12 h at 430 K in dry nitrogen atmosphere and—similar to the procedure in the ellipsometry experiments—directly measured without exposing the sample to ambient air. The recorded spectra of dielectric loss  $\epsilon''$  show a strong  $\beta$ -relaxation peak which superimposes the much weaker  $\alpha$ -relaxation. The reduced amount of sample material in the capacitor when measuring thinner layers leads to a decreasing signal intensity. Nevertheless, in temperature representation (which is fully equivalent to a frequency representation) at lower frequencies ( $\sim 120$  Hz) the  $\alpha$ -relaxation occurs well separated from the stronger  $\beta$ -relaxation. In such a representation one obtains the characteristic temperature  $T_\alpha$  at the chosen frequency, which

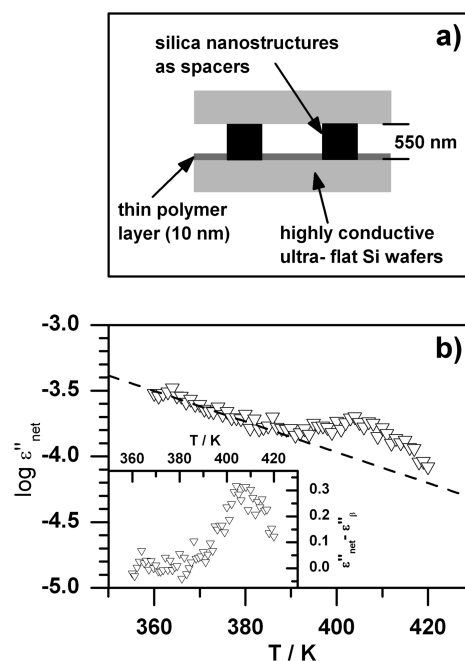


**Figure 2.** Upper sketch (a) shows the sample geometry applied for the BDS measurements where highly conductive and ultraflat silicon wafers are used as electrodes while nanostructures 550 nm high serve as spacers. The imaginary part of the net dielectric function  $\epsilon''_{\text{net}}$  measured at a frequency of 120.74 Hz for a 12 nm thin PMMA layer in this geometry is plotted in (b). The dashed line indicates the interpolation of the wing of the  $\beta$ -relaxation whose subtraction delivers the contribution of the  $\alpha$ -relaxation as seen in the inset.

corresponds to a relaxation rate at this temperature. Although the  $\alpha$ -relaxation peak appears separately from the  $\beta$ -relaxation in the graph of Figure 2b, the wing of the latter affects the shape of the curve of the  $\alpha$ -peak, thereby introducing a shift of the maximum position. This contribution was eliminated by interpolating the wing of the  $\beta$ -relaxation and subtracting this curve from the data (Figure 2b, inset).

For both ellipsometric and dielectric measurements, atomic force microscopy (AFM) was always applied to check the surface morphology of the samples before and after measurement. The root-mean-square roughness was observed to remain always below 3 nm. This observation implies the exclusion of any dewetting of the polymer which could, otherwise, mimic or conceal confinement effects. Furthermore, for the dielectric studies, AFM was used to determine the thickness of the layers. To do this, the polymer sample was scratched without harming the substrate (as checked by AFM) and the height of the resulting step measured at 15 positions. Averaging these values gives the mean sample thickness within a variability of  $\pm 10\%$  for layers down to  $\sim 20$  nm and up to  $\pm 20\%$  for thinner samples. Additionally, the reproducibility of the measurements was always checked. For ellipsometry, several heating and cooling cycles were carried out on the samples after annealing and the data recorded as shown in Figure 3a (only one cycle is shown for graphical clarity since the curves completely coincide). Similarly, for BDS the dielectric loss as a function of temperature was monitored (after annealing) before and after measurement (Figure 3b). For both techniques, good reproducibility was ascertained, and hence metastable states from nonequilibrated samples which could mimic confinement effects are excluded.<sup>2</sup>

### 3. Results and Discussion

**3.1. Ellipsometric Measurements.** All measured samples exhibit a discontinuity (“kink”) in the monitored thickness  $d$  and refractive index  $n$  in the investigated temperature range. Figure 4a exemplifies this observation in the case of spin-cast

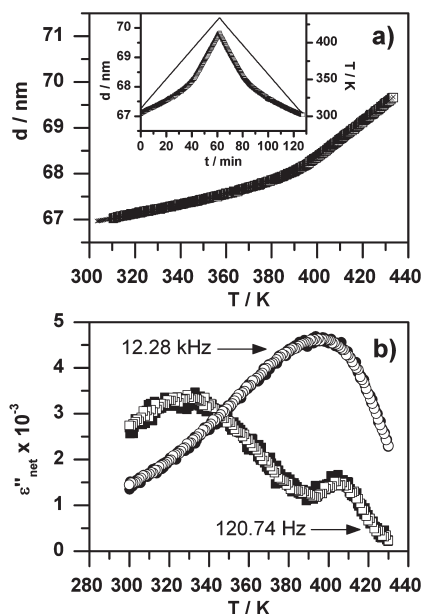


**Figure 3.** Graph (a) shows the ellipsometrically determined thickness  $d$  of a 67 nm thin PMMA sample on Si/SiO<sub>x</sub> during a typical heating (open squares) and cooling (crosses) cycle. In the inset the time dependence of these thickness measurements (open squares) and the corresponding temperature (solid line) are plotted. The temperature dependence of the net dielectric loss  $\epsilon''_{\text{net}}$  of a 30 nm thin PMMA layer on Si/SiO<sub>x</sub> as recorded before (solid symbols) and after (open symbols) the main dielectric measurement (both carried out after annealing) at two different frequencies as indicated is presented in (b). In both ellipsometric and dielectric experiments, the coincidence of the curves proves reproducibility of the measurements.

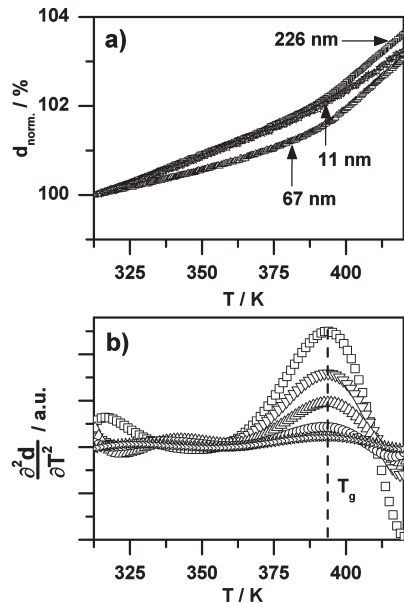


**Figure 4.** Normalized layer thickness ( $d/d_0 \times 100\%$ , with  $d_0$  as the initial thickness at 310 K) for thin PMMA layers on Si/SiO<sub>x</sub> having thicknesses as indicated (a). (For reasons of clarity only three curves are shown.) Variations in slope are due to small differences in thermal expansion. The second derivatives of the interpolated  $d(T)$  curves are shown in (b) for layers as thick as 11 nm (stars), 26 nm (circles), 67 nm (up triangles), 112 nm (down triangles), and 226 nm (squares). The maximum indicates the glass transition temperature.

PMMA layers supported on the native oxide surface of silicon wafers. The exact position of this discontinuity (Figure 4b), indicating the ellipsometrically determined glass

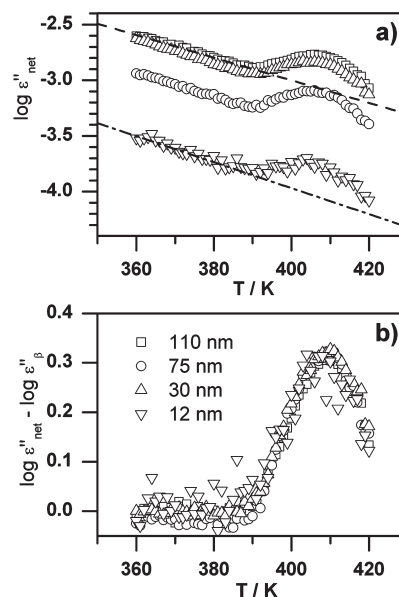


**Figure 5.** Net dielectric loss  $\epsilon''_{\text{net}}$  versus temperature at a frequency of 120.74 Hz of PMMA layers on Si/SiO<sub>x</sub> surfaces having a thickness of 12 nm (down triangles), 30 nm (up triangles), 75 nm (circles), and 110 nm (squares) (a). These graphs were adjusted by subtracting the contribution of the  $\beta$ -relaxation (linear interpolation of the wing, exemplified by the dashed and dash-dotted lines for the case of 110 and 12 nm thick layers) to obtain corrected curves which represent the  $\alpha$ -relaxation (b).

transition temperature  $T_g$ , was determined as described in section 2.2. No thickness dependence of  $T_g$  is exhibited by the PMMA layers spin-cast on *any* of the applied substrates in the studied thickness range (11–723 nm on Si/SiO<sub>x</sub>, 33–225 nm on gold-coated Si/SiO<sub>x</sub>, and 14–245 nm on silanized Si/SiO<sub>x</sub>; see Figure 6, parts a, b, and c, respectively). Further, no deviation from the calorimetrically (DSC) determined bulk  $T_g$  occurs.

The PMMA brushes, i.e., polymer chains covalently tethered on Si/SiO<sub>x</sub>, exhibit an ellipsometrically determined  $T_g$  which is raised by about 3 K compared to the  $T_g$  of the non-tethered PMMA. But also in this unique polymer conformation, no thickness dependence is observed in the investigated PMMA brushes, ranging from 25 to 119 nm (Figure 6d).

**3.2. Dielectric Measurements.** In the investigated frequency and temperature range, PMMA exhibits an  $\alpha$ -relaxation peak and a wing of the much stronger  $\beta$ -relaxation. In the chosen temperature representation of the dielectric loss  $\epsilon''$  at a frequency of 120.74 Hz, the  $\alpha$ -relaxation occurs at higher temperatures and separately from the  $\beta$ -relaxation. The impact of the high temperature wing of the latter was eliminated as described in section 2.2, and thus the dielectric loss caused by the  $\alpha$ -relaxation is obtained. Figure 5 exemplifies these findings in the case of PMMA layers spin-cast on Si/SiO<sub>x</sub>. No shift of  $T_\alpha$  measured at a frequency of 120.74 Hz is found in the studied thickness range, regardless of the substrate (12–350 nm on Si/SiO<sub>x</sub>, 19–221 nm on gold-coated Si/SiO<sub>x</sub>, and 37–350 nm on silanized Si/SiO<sub>x</sub>; see Figure 6, parts a, b, and c, respectively).

Figure 6 summarizes the previously discussed results and shows that (a) no thickness dependence of the ellipsometrically determined  $T_g$  and the dielectrically determined  $T_\alpha$  is exhibited by PMMA layers spin-cast on Si/SiO<sub>x</sub>, gold-coated or silanized Si/SiO<sub>x</sub> surface; (b) in the investigated thickness range of the spin-cast samples no impact of the substrate on the ellipsometrically determined  $T_g$  and the dielectrically determined  $T_\alpha$  is detected; (c) the ellipsometrically determined values



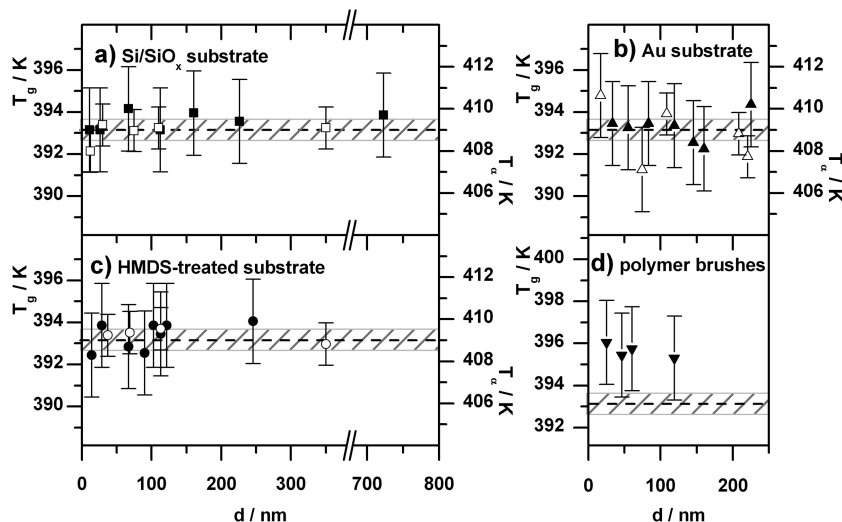


**Figure 6.** Glass transition temperature  $T_g$  measured by ellipsometry (filled symbols) and characteristic temperature  $T_\alpha$  (at 120.74 Hz) measured by BDS (open symbols) plotted versus layer thickness  $d$ . The measurements were carried out on different substrates having hydrophilic (a, Si/SiO<sub>x</sub>) to hydrophobic (b, gold coating; c, silanized with HMDS) surfaces. Additionally, covalently bonded PMMA brushes on Si/SiO<sub>x</sub> with strong attractive interfacial interactions were studied (d). The calorimetrically determined  $T_g$  of the bulk is shown by dashed lines, and the experimental error of  $\pm 0.5$  K (shaded region) is plotted for comparison.

of  $T_g$  coincide with the bulk  $T_g$  (DSC); and (d) the ellipsometrically determined  $T_g$  of PMMA brushes covalently tethered on Si/SiO<sub>x</sub> is increased by about 3 K compared to the non-tethered, but again *no* thickness dependence is revealed.

For a discussion of these results in the context of the literature, first of all, it is important to note that the glassy dynamics of PMMA varies strongly with tacticity,<sup>7,25,26</sup> this might be due to the fact that tacticity introduces a structural length scale, namely, the number of chain segments building a block of a certain tacticity. This implies that the length scale where possible confinement effects are expected depends on the tacticity as well.<sup>9</sup> Thus, studies reporting on atactic PMMA are of major interest for our discussion.

To the best of our knowledge, there are only few studies concerning the glassy dynamics in thin layers of atactic PMMA. Some of them, carried out by BDS and DSC, do not find any shift of the glassy dynamics<sup>9,27,28</sup> while others, mainly using ellipsometry, observe changes in  $T_g$  as big as 5–10 K in 40–20 nm thick layers.<sup>7,10,17,29</sup>

It is known that remaining solvent in polymers can have plasticizer effects and metastable states can occur in non-equilibrated samples, both of which factors lead to altered glassy dynamics.<sup>2,3,30</sup> Consequently, a proper annealing procedure (at a temperature well above  $T_g$  for sufficient long time in an inert oxygen- and water-free atmosphere) is essential to obtain robust results.<sup>2,3</sup> A close look at the cited studies shows that in some cases the ambience of either annealing<sup>7,9</sup> or the measurement itself<sup>7,9,10,17,29</sup> is not mentioned. For instance, in the seminal paper by Keddie and Jones<sup>10</sup> the annealing is properly done, but no comment is made concerning the ambient conditions during the measurement itself. In a similar study on polystyrene,<sup>31</sup> the same authors did measurements in ambient air; it is therefore likely that the same ambience was used in their work<sup>10</sup> on PMMA. Considering these preparative and experimental differences, the corresponding results seem to represent the impact of some kind of a preparative history on the glassy dynamics rather than a size or confinement effect. The fact that some studies do not find thickness dependent shifts of the glassy dynamics<sup>9,27,28</sup> implies that in these cases the preparative and experimental conditions were sufficient to avoid effects on the glassy dynamics of the polymer layers, as is the case in the present investigation.

#### 4. Conclusion

In the present study, the impact of geometrical confinement in thin layers and differently interacting substrates on the glassy dynamics of atactic PMMA is investigated by means of ellipsometry and BDS. Within the limits of experimental accuracy ( $\pm 2$  K for ellipsometry and  $\pm 1$  K for BDS) *no* shift of the glassy dynamics is detected neither by decreasing the thickness of the polymer layer nor by changing the type of the substrate interaction from covalently bonded (brushes) through hydrophilic (Si/SiO<sub>x</sub>) to weakly and strongly hydrophobic (gold-coated and silanized Si/SiO<sub>x</sub>, respectively).

Considering the conflicting reports in the literature and the corresponding preparative and experimental facts which we have discussed, we conclude that sample preparation is the major factor leading to the observation of altered glassy dynamics in thin polymer layers. At this point, we would like to emphasize that in the present study the results of two different experimental approaches—ellipsometry and BDS—are combined and were carried out in full independence by two different groups. The only common ground consisted in the identical annealing and measurement conditions which were implemented in both laboratories independently.

**Acknowledgment.** The authors thank E. Schierz and R. Schulze for their manifold support and fruitful discussions. We greatly acknowledge the financial support of DFG (EI 317/4-1 and SPP1369).

#### References and Notes

- (1) Serghei, A.; Huth, H.; Schellenberger, M.; Schick, C.; Kremer, F. *Phys. Rev. E* **2005**, *71*, 061801.
- (2) Serghei, A.; Kremer, F. *Macromol. Chem. Phys.* **2008**, *209*, 810.
- (3) Serghei, A.; Kremer, F. In *Progress in Colloid and Polymer Science*; Grundke, K., Stamm, M., Adler, H.-J., Eds.; Springer: Berlin, 2006; pp 33–40.
- (4) Roth, C. B.; Pound, A.; Kamp, S. W.; Murray, C. A.; Dutcher, J. R. *Eur. Phys. J. E* **2006**, *20*, 441.
- (5) Dalnoki-Veress, K.; Forrest, J.; Murray, C.; Gigault, C.; Dutcher, J. *Phys. Rev. E* **2001**, *63*, 031801.
- (6) Karasz, F. E.; MacKnight, W. J. *Macromolecules* **1968**, *1*, 537.
- (7) Grohens, Y.; Brogly, M.; Labbe, C.; David, M.-O.; Schultz, J. *Langmuir* **1998**, *14*, 2929.
- (8) Wübbenhorst, M.; van Turnhout, J. *J. Non-Cryst. Solids* **2002**, *305*, 40.

- (9) Fukao, K. *Eur. Phys. J. E* **2003**, *12*, 119.
- (10) Keddie, J. L.; Jones, R. A. L.; Cory, R. A. *Faraday Discuss.* **1994**, *98*, 219.
- (11) Reiter, G. *Macromolecules* **1994**, *27*, 3046.
- (12) Forrest, J. A.; Dalnoki-Veress, K.; Stevens, J. R.; Dutcher, J. R. *Phys. Rev. Lett.* **1996**, *77*, 2002.
- (13) van Zanten, J. H.; Wallace, W. E.; Wu, W. L. *Phys. Rev. E* **1996**, *53*, R2053.
- (14) Forrest, J. A.; Dalnoki-Veress, K. *Adv. Colloid Interface Sci.* **2001**, *94*, 167.
- (15) Roth, C. B.; Dutcher, J. R. *J. Electroanal. Chem.* **2005**, *584*, 13.
- (16) Alcoutlabi, M.; McKenna, G. B. *J. Phys.: Condens. Matter* **2005**, *17*, R461.
- (17) Fryer, D.; Nealey, P.; Pablo, J. *Macromolecules* **2000**, *33*, 6439.
- (18) Sharp, J. S.; Forrest, J. A. *Phys. Rev. E* **2003**, *67*, 031805.
- (19) Kremer, F.; Schönhals, A. In *Broadband Dielectric Spectroscopy*; Kremer, F., Schönhals, A., Eds.; Springer: Berlin, 2003.
- (20) Erber, M.; Khalyavina, A.; Eichhorn, K.-J.; Voit, B. I. *Polymer* **2010**, *51*, 129.
- (21) Prucker, O.; Christian, S.; Bock, H.; Rühle, J.; Frank, C. W.; Knoll, W. *Macromol. Chem. Phys.* **1998**, *199*, 1435.
- (22) Whiting, G. L.; Farhan, T.; Huck, W. T. S. In *Polymer Brushes*, 1st ed.; Advincula, R. C., Brittain, W. J., Caster, K. C., Rühle, J., Eds.; Wiley-VCH: Weinheim, 2004; Vol. 18, p 371.
- (23) Serghei, A. *Macromol. Chem. Phys.* **2008**, *209*, 1415.
- (24) Serghei, A.; Kremer, F. *Rev. Sci. Instrum.* **2008**, *79*, 026101.
- (25) Grohens, Y.; Hamon, L.; Reiter, G.; Soldera, A.; Holl, Y. *Eur. Phys. J. E* **2002**, *8*, 217.
- (26) Wübberhorst, M.; Murray, C.; Forrest, J.; Dutcher, J. In *Proceedings of the 11th International Symposium on Electrets*; Fleming, R., Ed.; IEEE Service Center: Piscataway, NJ, 2002; pp 401–406.
- (27) Efremov, M. Y.; Olson, E. A.; Zhang, M.; Zhang, Z.; Allen, L. H. *Phys. Rev. Lett.* **2003**, *91*, 085703.
- (28) Efremov, M.; Olson, E.; Zhang, M.; Zhang, Z.; Allen, L. *Macromolecules* **2004**, *37*, 4607.
- (29) Fukao, K.; Uno, S.; Miyamoto, Y.; Hoshino, A.; Miyaji, H. *Phys. Rev. E* **2001**, *64*, 051807.
- (30) Labahn, D.; Mix, R.; Schönhals, A. *Phys. Rev. E* **2009**, *79*, 011801.
- (31) Keddie, J. L.; Jones, R. A. L.; Cory, R. A. *Europhys. Lett.* **1994**, *27*, 59.